

Fluid inclusion studies of mineralized zones of Kudrekonda, Kodikoppa and Palavanahalli, Honnali Gold deposit in Shimoga schist belt, Western Dharwar Craton

Shivaprasad R., Ananthamurthy K.S. and Shashikala C.

Department of Applied Geology, Kuvempu University, Shankaraghatta, 577 451, India
shivaprasad341986@gmail.com

Available online at: www.isca.in

Received 4th May 2017, revised 2nd June 2017, accepted 18th June 2017

Abstract

The general properties of fluid inclusions in hydrothermal ore-forming systems are considered and the interpretation of these data in terms of fluid evolution processes is discussed. The Honnali gold deposit is located at the southern part of the Shimoga schist belt. The characteristics of ore-forming fluids and metallogenesis were discussed by using fluid petrography, micro-thermometry. All three types of inclusions, mainly type I having homogenization temperatures at 16 to 28°C, and salinities ranging from 1.49 to 5.32 Wt% NaCl_{eqv}. The initial ice melting temperatures (T_{FM}) range from -56.6 to -56.7°C. This implies that the major component in aqueous phase is NaCl dominated with NaCl ± KCl and H₂O in the fluid system. Primary carbonic fluid inclusions in these samples are typically mono-phase at room temperature. The type-II, the melting temperature of CO₂ range from -56.6°C to -57.2°C indicating that the fluid dominated by CO₂ and the maximum depression of melting temperature of CO₂ is -57.2°C (Table-1), indicating the fluid contains CO₂ with very minor amount volatile gases such as (i.e. CH₄/N₂). Type -III, the final melting temperature of ice ranges from -12 to -0.3°C which corresponds to a salinity range of 0.5 to 15.76 Wt% NaCl equivalent, Application of standard criteria for the recognition of primary, pseudo-secondary and secondary inclusions is essential. Furthermore, as stated by Roedder and Bodnar, most inclusions in most samples can be presumed to be secondary, unless proved otherwise.

Keywords: Honnali gold field, Geology, Fluid inclusion petrography, Microthermometric data, P-T conditions of mineralization, Fluid source of gold.

Introduction

H.C. Sorby first proposed the use the term "Fluid Inclusion" for deciphering the temperature of past geological events¹. Fluid inclusions have provided much information that has been used in many ways in the mineral exploration and in problem of understanding the physical and chemical events of ore deposition. Fluid inclusions trapped in minerals provide information on the temperature, pressure and fluid composition attending various geologic processes². Over the years a standard methodology has been developed and accepted by the scientific community for the collection and interpretation of data from fluid inclusions³. The first and most important step in the process is to identify a Fluid Inclusion Assemblage (FIA), defined as the most finely discriminated fluid inclusion trapping event that can be identified based on petrography⁴. This definition implies that the fluid inclusions in the assemblage all trapped a fluid of the same composition "at the same time" and, by extension, at the same temperature and pressure⁵.

Fluid inclusions were classified based on the orientation of fluid inclusions within the mineral into primary and pseudo-secondary inclusions following⁶. Fluid inclusions were classified into Isolated Fluid Inclusions (IFI), which are primary

inclusions in minerals and Trail Bound Inclusions (TBI), which are intragranular, fracture - bound secondary inclusions in minerals. Based on the distribution pattern of inclusions, the isolated inclusions are classified as Group of Synchronous Inclusions (GSI)⁷. The term GSI to describe the trail bound inclusions in quartz grains. Care has been taken to record the textural relationship between fluid inclusions and the host mineral to document the relative timing of fluid entrapment which is a prerequisite for meaningful interpretation of fluid inclusion data⁸.

Few previous studies on deposit characteristics, mineral resources of Honnali gold field haven't been reported, and its metallogenic mechanism, especially as it pertains to the characteristics of ore fluids, remain unclear. An investigation of the metallogenic mechanism and the evolution of the ore fluids are important for ore exploration and understanding the ore-formation process. Fluid inclusions can provide abundant information on the genetic and evolutionary history of ore formation and thus play an important role in ore geology research⁹. This paper focuses on microthermometric studies of fluid inclusions from the main mineralization episode, with an aim to characterize the thermal and compositional evolution of

hydrothermal fluids and to discuss their implications for mineralization.

Geological setting

The terminology Dharwar Craton was first proposed by and summarised its geology under the same title¹⁰⁻¹². The Dharwar craton is one of classical and well-studied Archaean granite greenstone terrains of the world and is principally composed of low k-tonalitic to trondhjemitic gneisses (Peninsular gneiss) with infolded supracrustal (Sargur group) and capped by younger series of volcano sedimentary sequences (Dharwar super group). The strong N-S trending fabric of the Dharwar craton is partly due to late Archaean transcurrent shearing episode and is contemporaneous with the emplacement of Closepet granite¹³⁻¹⁵. The craton is divided into two tectonic blocks as Western and Eastern block¹⁶ and renamed respectively as Western Dharwar Craton (WDC) and Eastern Dharwar craton (EDC) and separated by Chitradurga shear zone situated to the west of the linear Closepet granite¹⁷. The schist commonly referred as greenstones include metavolcanic and metasedimentary rocks of clastic/chemical origin. These schistose rocks occur as narrow elongated belts in the peninsular gneisses and have been termed as greenstone belts. The greenstone belts occurring to the east and west of closepet granite are grouped as i. eastern greenstone belts and ii. western greenstone belts. Kudrekonda-Palavanahalli, also described as the Honnali Gold Field¹⁸. An auriferous zone is traceable along the southwestern margin of the Honnali granite dome and northeastern margin of the Saulanga granite both of which occur within the Shimoga schist belt (Figure-1). The structure of the Shimoga schist belt is characterized by southwest verging folds in the Dharwar schists and by north dipping reverse faults forming the southern boundaries of basement domes like Tarikere, Honnali and Shimoga. The rocks of the Shimoga greenstone belt have suffered greenschist to amphibolite grade of metamorphism and rest over gneissic basement that are exposed at Honnali, Soulanga and Shimoga. The Study area is located in the southernmost part of the Shimoga schist belt. The northern boundaries of these domes represent unconformities steepened by folding. Horizontal sinistral displacement is noticed in some shear zones. The basement gneisses on the other hand, are deformed in myriad brittle fracture as well as ductile, mylonitic shear zones. Abundant carbonates seen in fractures attest to the role of CO₂ activity. The evolution of Shimoga belt is governed by sinistral transgression in an ensialic-slip mobile zone¹⁹. Variably intense LS fabrics formed with the Haramaghatta-Nallinakoppa syncline. The principal S fabric is a mixed pressure solution and crenulation cleavage.

Geology of Kudrekonda-KK, Kodikoppa-KDK and Palavanahalli-P

The Study area is located in the southernmost part of the Shimoga schist belt. Geographically the area extends from 75°30'30"E to 75°40'E longitude and 14°5'50"N to 14°10'N

latitude. Kudrekonda-Palavanahalli, also described as the Honnali Gold Field³¹. An auriferous zone is traceable along the southwestern margin of the Honnali granite dome and northeastern margin of the Saulanga granite both of which occur within the Shimoga schist belt. Surface soil and gravel, especially in the region Kudrekonda, Palavanahalli, Surahonne and Nyamati at the south western margin of the Honnali granite dome, contain coarse particles of gold²¹. A mottled assemblage of schistose rocks form the narrow range of the study area, bordered on the western side by the Saulanga granite and on the eastern by the Honnali granite. The schistose rocks, in between these two granites, are composed of a thick series of acid and basic lava flows, conglomerates and a number of bands of quartzites with intercalated argillitic material. The rocks have all a general NNW-SSE strike and dip regularly towards the east. Parallel with this general strike number of a series of quartz veins on which are situated a number of old workings for gold. A well-developed zone of conglomerate and quartzite forms the southwestern extent of the Honnali dome where old workings are located at the foot of the Kalavarangetta mountain range²². The quartzites and conglomerates on account of their weather-resisting qualities stand out in the form of bold line of hills (Figure-2).

Kudrekonda: The volcano-sedimentary sequence overlying the basement granodiorite and gneisses in the Honnali dome were labeled as Kudrekonda formation⁵. They have proposed that association of metabasalts, orthoquartzite, quartz sericite schist, acid volcanic and phyllites at the base of Dharwar super group flanking the Honnali dome be labeled as the Kudrekonda formation after the area that includes the disused gold workings. They also proposed Kalva Rangan Durga formation for the large scale intercalation of orthoquartzite, conglomerate, cherts and phyllites, which exposed in Kalva Rangan hill ranges. Amphibole occurs as major litho-units, undergone upper green schist to lower amphibole facies metamorphism and host rock for auriferous quartz veins. The contact between the Kudrekonda formation and the basement gneiss is exposed at about 3 Km west of Somanna Mallapur with schistose, feldspathic, locally pebbly quartzite or arkose as the basement. Following is the stratigraphic succession established for the south and southwestern portion (Kudrekonda area) flanking the Honnali dome³.

Kodikoppa: Kodikoppa zone located between Kudrekonda and Palavanahalli area, occupied by completely weathered quartz chlorite schist with general strike NNW-SSE, covered by soil. kodikoppa mineralized zone is situated at 1.5 Km of Kodikoppa village in a nalha cutting at 1 Km south of Nymathi. Two quartz veins samples were collected from tourmaline bearing white sacchroidal quartz vein indicated high Au values. Around 108m long and 0,2 to 2.2m wide auriferous quartz vein.

Palavanahalli: Palvanahalli prospect is located at 6.5 km south Nyamathi and it is a southeastern extension of Kudrekonda and Kodikoppa prospects The area under investigation forms

southern part of the Dharwar- Shimoga schist belt in the western Dharwar craton. The tract is characterized by a series of parallel disposed, NNW –SSE trending ridges are composed essentially of dark green quartz chlorite schist and altered basalts in which numerous thin veins of quartz are traversed. Mineralization occurs in intensely altered metabasalts. A large part of this mineralization is covered by a blanket of soil.

In this region two zones of gold mineralization have been identified by author. Mineralized zones are characterized by sheeted chalcidony ± calcite veins traversing silicified, sulphide, and hydrothermally altered basalt. Around Palavanahalli numerous bands of quartzite are exposed which are highly folded, contorted and broken up and which have the character of coarse sandstones approaching pebbly beds.

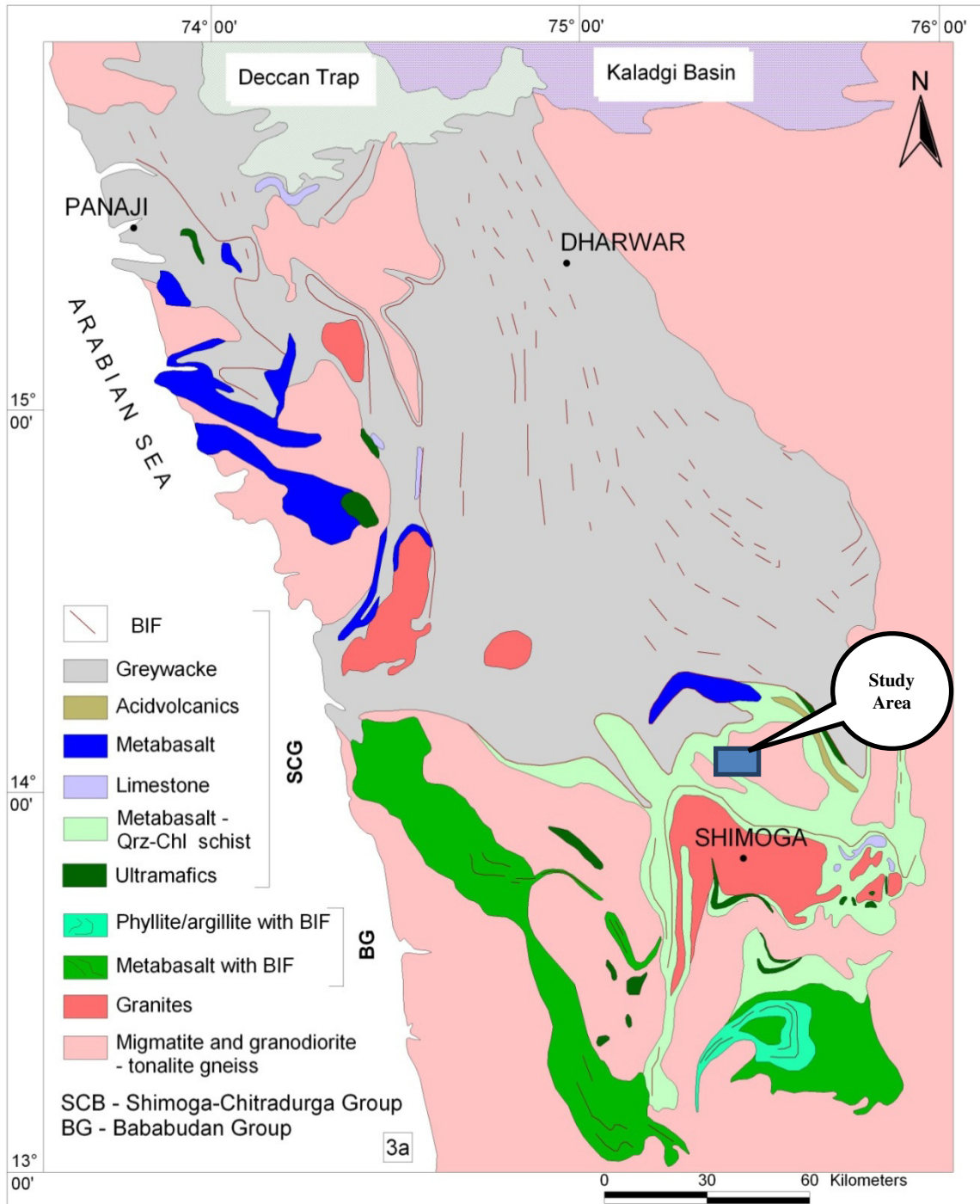


Figure-1: Geology Map of Shimoga Schist Belt (Radhakrishna and Vaidyanadhan, 1997)²⁰.

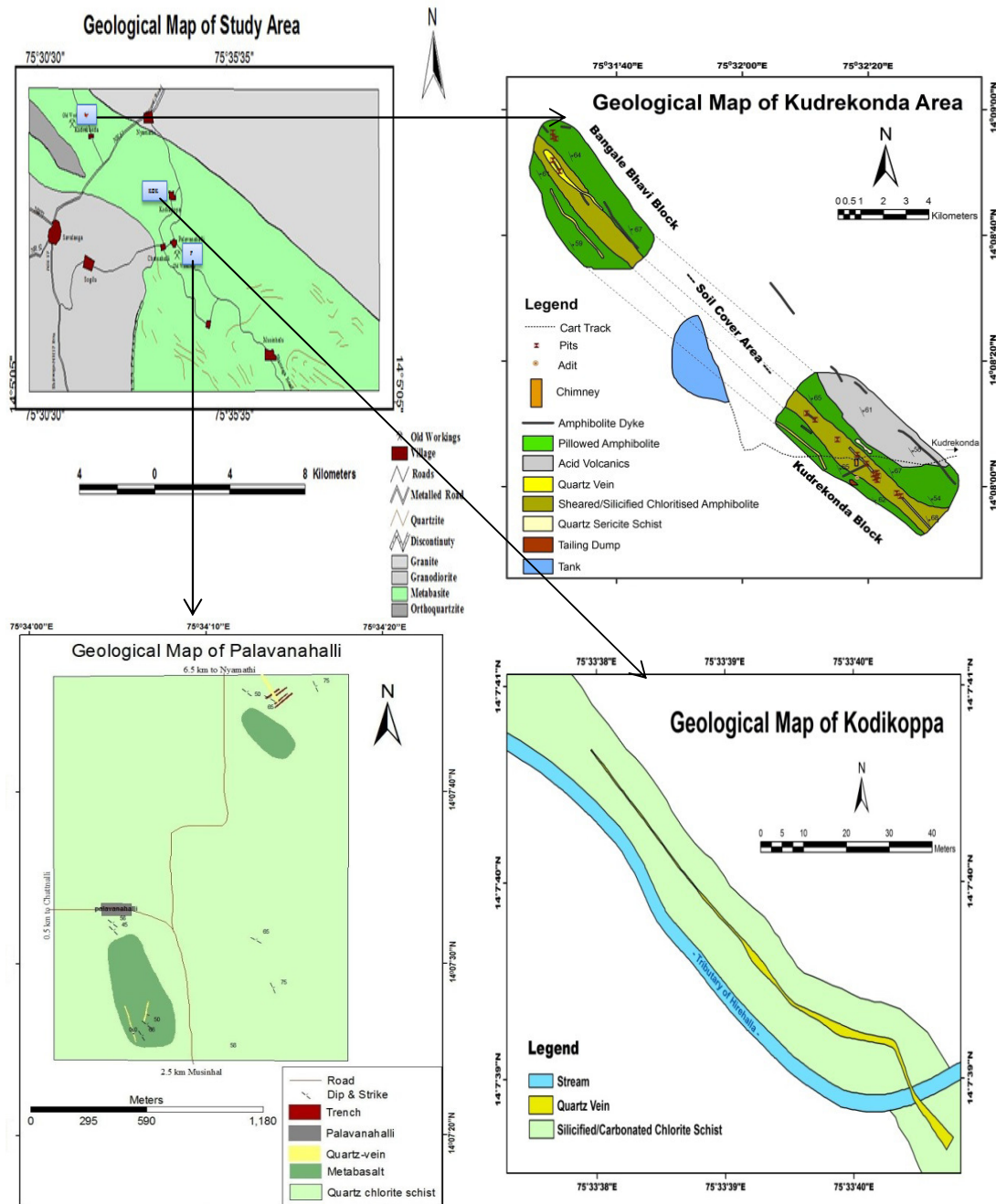


Figure-2: Geology map of the Study area.

Sample selection and preparation

Doubly polished thin wafers for 3 samples were prepared after preliminary study of thin sections. Doubly polished 300-350 μm thick wafers were prepared to characterize the fluid inclusions and used for microthermometric investigations.

Fluid inclusion petrography

Doubly polished thin wafers from each sample were prepared for fluid inclusions studies. Petrographic studies of wafers

indicate the presence of primary and secondary mono-phase/bi-phase inclusions in one sample. The size of the vapor phase in the form of bubble ranges from 0.12 to 1.76 μm . The characters of the bubble indicate heterogeneous nature of the parent fluid. These inclusions are generally small irregular and faceted (Figure-1 and 2). The size of inclusions varies from 0.72 to 17.17 μm .

Primary bi-phase isolated inclusions are of various shapes (oval, spherical, rounded, and irregular and faceted) (Figure-1 and 2).

Secondary inclusions are smaller in sizes and are rounded and faceted in shapes. They occur linearly along healed fractures. Carbonic inclusions occur nearby near in the samples (Figure-3). The study of wafers indicate that the area occupied by the vapor phase ranges from 1 to 30%. The area occupied by the aqueous phase varies from 71 to 99% (average 88%). Carbonic inclusions are also present in these wafers.

All the Fluid inclusion assemblages (primary and secondary) were scanned thoroughly in all the eight wafers and only prominent inclusions were selected for detail micro thermometric study. The size of inclusions varies between 0.72 to 17.17 μm . Few CO_2 vapor bubbles show a dark rim in the periphery at room temperature, which is due to the presence of a thin film of liquid CO_2 trapped inside vapor CO_2 .

Instrument and Methodology

The microthermometric studies were carried out using Linkan THMSG 600 heating and freezing stage fitted with Olympus BX 50 transmitted light microscope. A silver block (THMSB) is used for heating. The unit operates in the temperature range of -195° to $+600^\circ\text{C}$. The stage is periodically calibrated by using demineralised water (H_2O melting point = 0°C) and pure CO_2 inclusions (synthetic CO_2 standard of triple point = -56.6°C). Estimated accuracy is $\pm 0.1^\circ\text{C}$ at temperatures below 30°C and $\pm 1.00^\circ\text{C}$ at temperatures above 30°C . Reproducibility of the results of heating above 300°C has been tested and found to be ± 2 to 3°C .

Freezing experiments were performed first, on all the wafers to avoid the decrepitation of inclusions followed by heating²³. The measurements were carried out during final melting temperature of ice (T_{mice}) to determine the salinity of aqueous phase. During the heating of the fluid inclusions, homogenisation temperatures of the CO_2 (T_{hCO_2}) were measured to determine the density of CO_2 and the total homogenisation temperature (T_{hTotal}). Calculation of density, salinity of the inclusions and its plotting in the isochores of temperature and pressure were carried out by using Linksys software (version 1.8).

Fluid Inclusion Types

Three types of inclusions are noticed in studied samples. They are classified based on mode of occurrence and number of phases observed in room temperature. They are classified as follows; i. Aqueous carbonic (type-1), ii. Pure carbonic (type-II), iii. Aqueous (type-III).

Inclusions of aqueous carbonic (type-1): The observed range of homogenisation temperature varies from 16 to 28°C . The initial ice melting temperatures (T_{FM}) range from -56.6 to -56.7°C . This implies that the major component in aqueous phase is NaCl dominated with $\text{NaCl} \pm \text{KCl}$ and H_2O in the fluid system. The maximum of first ice melting temperature of -32°C may indicate the presence of $\pm \text{MgCl}_2$ with NaCl and H_2O ²⁴.

The final melting temperature of ice ranges from -3.3 to -0.9°C which corresponds to a salinity range of 1.49 to 5.32 Wt% NaCl equivale, calculated using Linksys software (version 1.8) following the equations of state given by many researchers^{1,2,48}. The density of aqueous phase studied varies from 0.68 - 0.86gms/cm^3 (Figure-1 and 2).

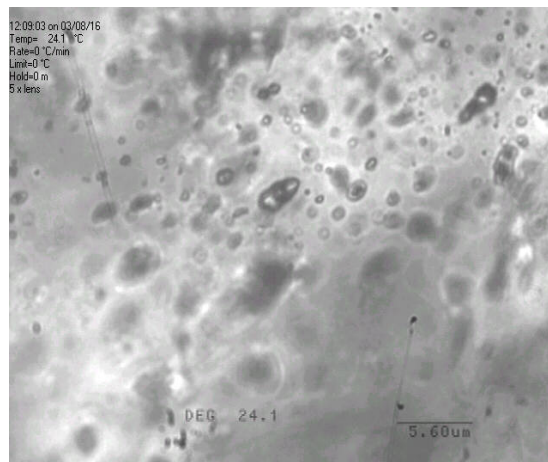


Figure-3: H_2O - CO_2 inclusions in KDK.

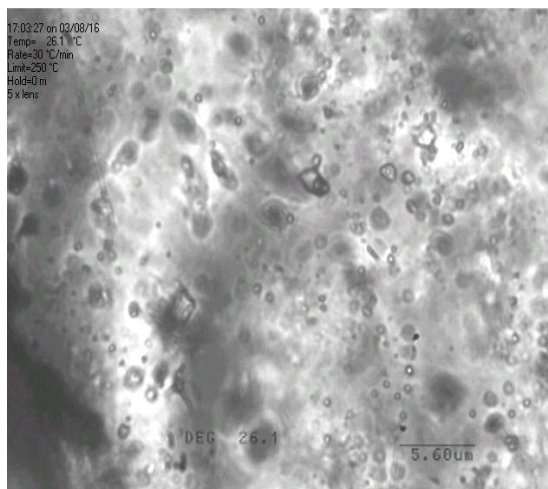


Figure-4: H_2O CO_2 inclusion in KK3.

Pure carbonic (type-2): Primary carbonic fluid inclusions in these samples are typically mono-phase at room temperature. During cooling experiments, a vapor bubble nucleates and homogenizes in to the liquid phase. The melting temperature of CO_2 range from -56.6°C to -57.2°C indicating that the fluid dominate by CO_2 and the maximum depression of melting temperature of CO_2 is -57.2°C (Table-1), indicating the fluid contains CO_2 with very minor amount volatile gases such as (i.e. CH_4/N_2). The homogenization temperature of CO_2 ranges from 15°C to 22°C . The isochors of carbonic inclusions is approximated by a CO_2 system indicate the variation in fluid pressures. The fluid pressures vary from 1300 to 1700 bars (Figure-16). The density of the CO_2 varies from 0.75 - 0.82g/cm^3 (Figure-3).

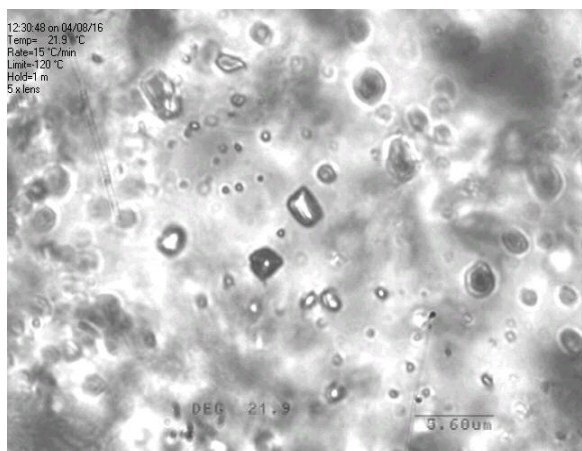


Figure-5: Pure Carbonic inclusion in KDK

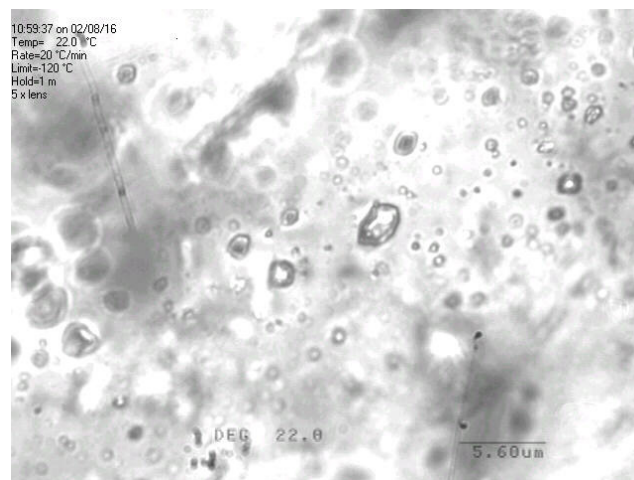


Figure-8: Aqueous inclusions.

Aqueous (type-3): The final melting temperature of ice ranges from -12 to -0.3°C which corresponds to a salinity range of 0.5 to 15.76 Wt% NaCl equivalent, calculated using Linksys software (version 1.8) following the equations of state given by many researchers²⁵⁻²⁷. The density of aqueous phase studied varies from 0.70gms/cm³ (Figure-4, 5 and 6).

Microthermometry: In general a normal rate of a 5°C/minute was maintained during thermometric runs, the melting of CO₂ and ice was checked repeatedly, doubtful inclusions showing necking or leakage were not used while presenting and interpreting the data. The freezing temperature found to be correct in the order of 0.2°C and heating runs were correct to 2°-3°C. The result of heating and freezing studies of fluid inclusions has been summarized in tabular form (Table-1).

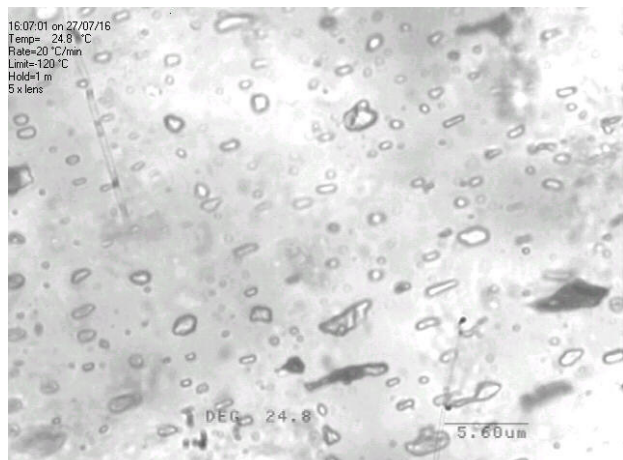


Figure-6: Aqueous inclusions.

First Melting Points of CO₂ (TmCO₂): CO₂ bearing inclusions were frozen to -110°C, then the inclusions were slowly heated to note the first melting points of CO₂ (Tm CO₂). The first melting temperature of CO₂ can be detected from observation of sudden phase changes of solid CO₂ in to liquid. The first melting point for pure CO₂ is known to be -56.6°C. Most inclusions show Tm CO₂ between -56°C to -57.2°C.

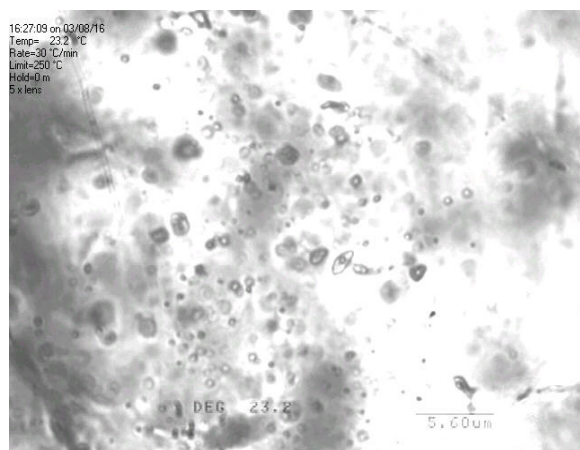


Figure-7: Aqueous inclusions.

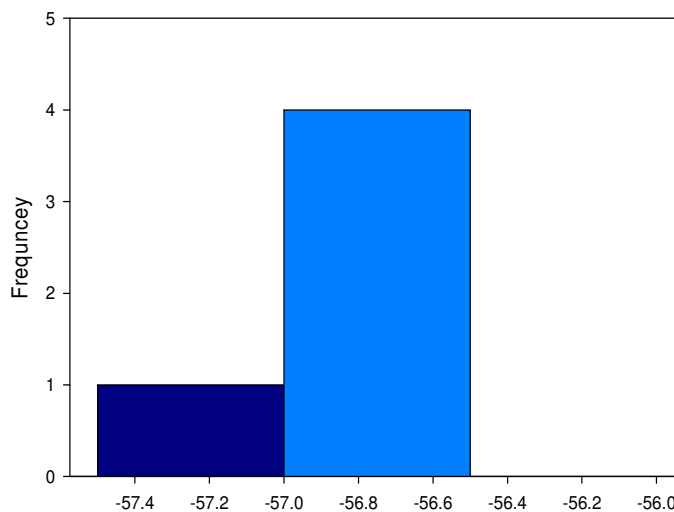


Figure-9: Histogram showing melting temperature (°C) of CO₂ in type-2 inclusions.

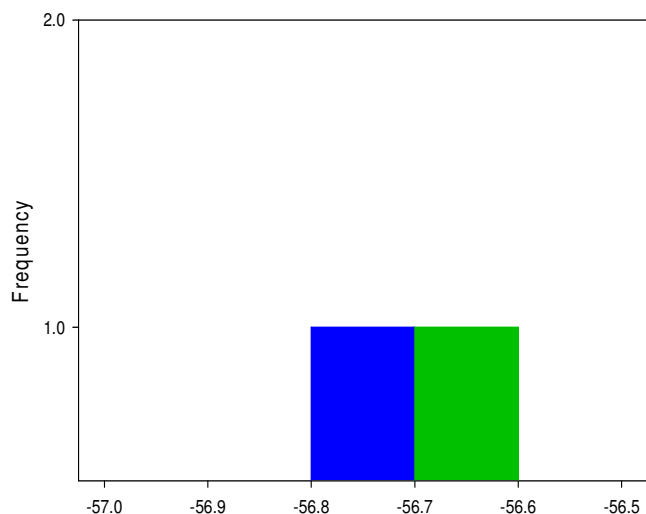


Figure-10: Histogram showing melting temperature (°C) of CO₂ in type-I inclusions.

Homogenization temperature of CO₂ (Th CO₂): After measuring the melting temperature of CO₂, further heating causes homogenization of liquid and gaseous CO₂ in to a single phase (Th CO₂). During the present study most of the inclusions homogenized into liquid phase. The temperature varying from 16 to 28°C and 15 to 22°C in type-I and II respectively.

Total homogenization temperature: Temperature of disappearance of gas phase was considered as temperature of homogenization. It is observed that all fluid inclusions homogenized to the liquid phase.

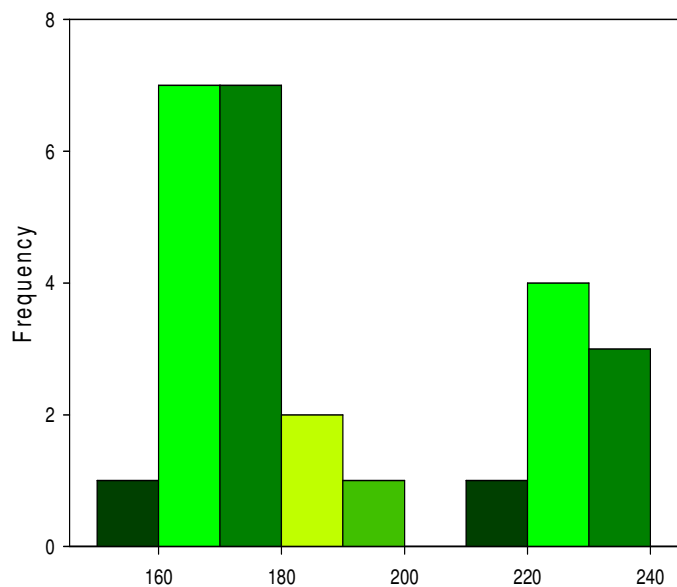


Figure-11: Th Total for type-3 inclusions.

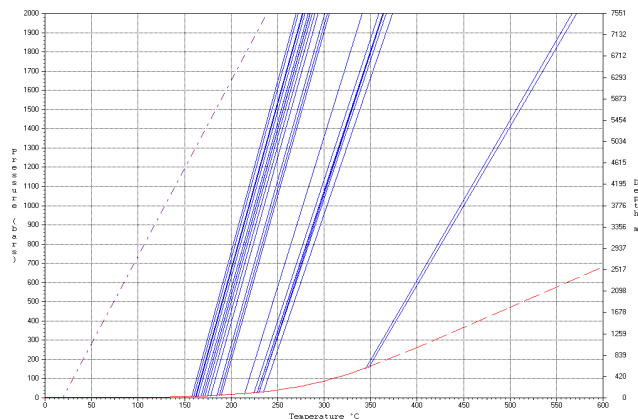


Figure-12: Temperature Isochores of aqueous fluid inclusions range between 158°C to 348°C.

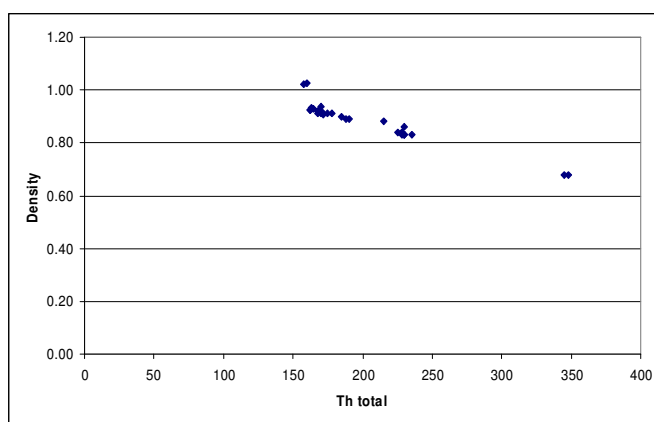


Figure-13: Plot showing Temperature of homogenization vs Density.

Salinity: Salinity of fluid is expressed as equivalent weight percent NaCl (wt % NaCl eq.). Final melting point of ice indicates salinity (wt% NaCl equivalent) of type-1 fluid inclusions. Final ice melting temperatures were used to determine for salinity of type-3 fluids.

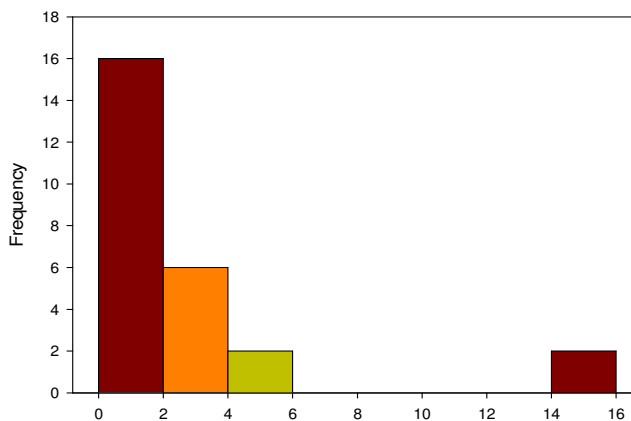


Figure-14: Type -3 inclusions.

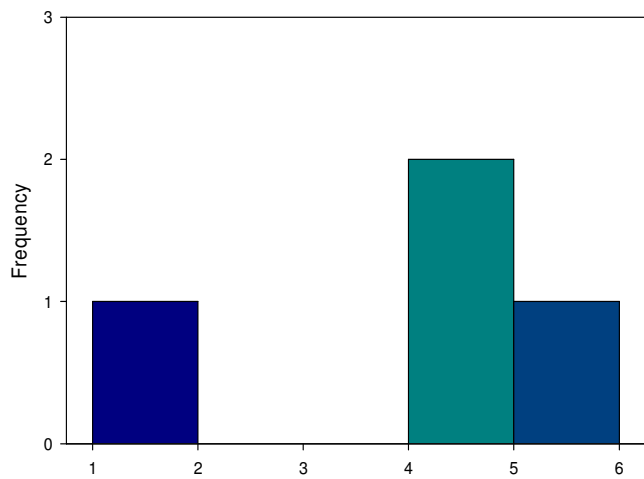


Figure-15: Type-1 Inclusions.

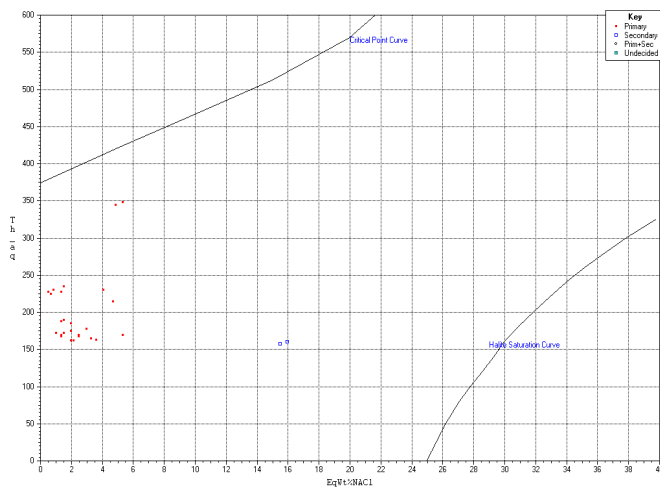


Figure-16: Plot of inclusions in Temperature of homogenisation vs Salinity field.

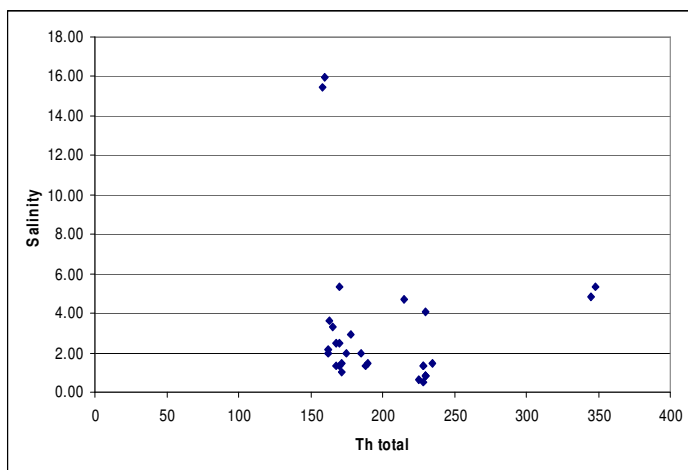


Figure-17: Plot showing Temperature of homogenization vs Salinity.

Density of CO₂: Equations given were applied to estimate CO₂ density based on H₂O-CO₂-CH₄ ternary system²⁸. The density calculation using the equation of state of Kerrick and Jacobs takes into account several other parameters (like the fraction of CO₂ present) than the homogenization temperatures of fluids, to determine the bulk density of the fluid²⁹. On the basis of these data fluid densities were estimated 0.68-0.86/ cm³ for type-1, 0.75-0.82g/cm³ for type-2, 0.70 cm³ for type-3 (Table-1).

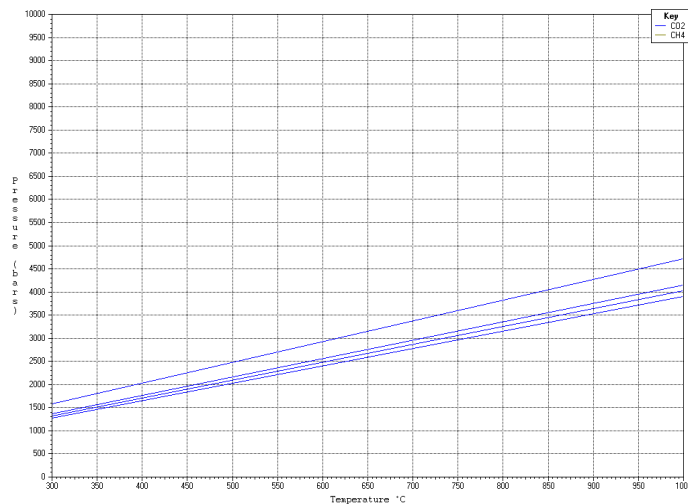


Figure-18: Density of CO₂.

Fluid source for gold: The studied samples contain fracture filled sulfide minerals in quartz vein. Thus fluid inclusions present in studied samples certainly represent a mineralizing event. Especially, less saline and H₂O-CO₂ fluids (type-1) in inclusions present in quartz veins is capable of transporting gold.

Extensive research on the Archaean lode gold deposits the world over shows that auriferous low salinity H₂O-CO₂ fluids were channelled up in transcrustal shear zones during the late stage of greenstone belt deformation and metamorphism. Thus during the late stage of Shimoga greenstone belt deformation and metamorphism, the circulating hydrothermal fluids (H₂O-CO₂ fluid) were responsible for the breakdown of ferromagnesian minerals and release of silica which along with gold from the tholeiite rocks formed the quartz veins within the shear zones.

This is correlated to the higher gold content available in the mafic rocks in general and also corroborated by the spatial proximity of the auriferous quartz veins to them. Thus the Shimoga greenstone belt constitutes orogenic gold deposits that formed by metamorphic fluids from accretionary processes and generated by prograde metamorphism and thermal re-equilibration of subducted volcano-sedimentary terrains. Recent work proposed Neoproterozoic active continental margin processes for the growth and evolution of continental crust in the Shimoga Greenstone Belt in western Dharwar Craton (Figure-16)³⁰.

Table-1: Summary of classification, properties and microthermometric data for fluid inclusions.

Fluid Inclusion Types	Type-1	Type-2	Type-3
Samples	In quartz vein	Quartz vein	Quartz vein
Size (µm)	5.02-17.18 µm	0.72-4.62 µm	0.72-11.72 µm
Melting temperature of solid CO ₂ T _m CO ₂ °C	-56.6 to -56.7°C	-56.6to -57.2°C	--
Homogenization temperature of CO ₂ Th CO ₂ °C	16 to 28°C	15 to 22°C	--
Temperature of final ice melt T _m Ice °C	-3.3 to -0.9 °C	--	-12 to -0.3°C
T _{htotal} °C	235 to 348°C	--	158 to 230°C
Density	0.68-0.86	0.75-0.82	0.70
Salinity Wt% NaCl.eqv.	1.49 to 5.32 Wt% NaCl.eqv.		0.5 to 15.76 Wt% NaCl.eqv.

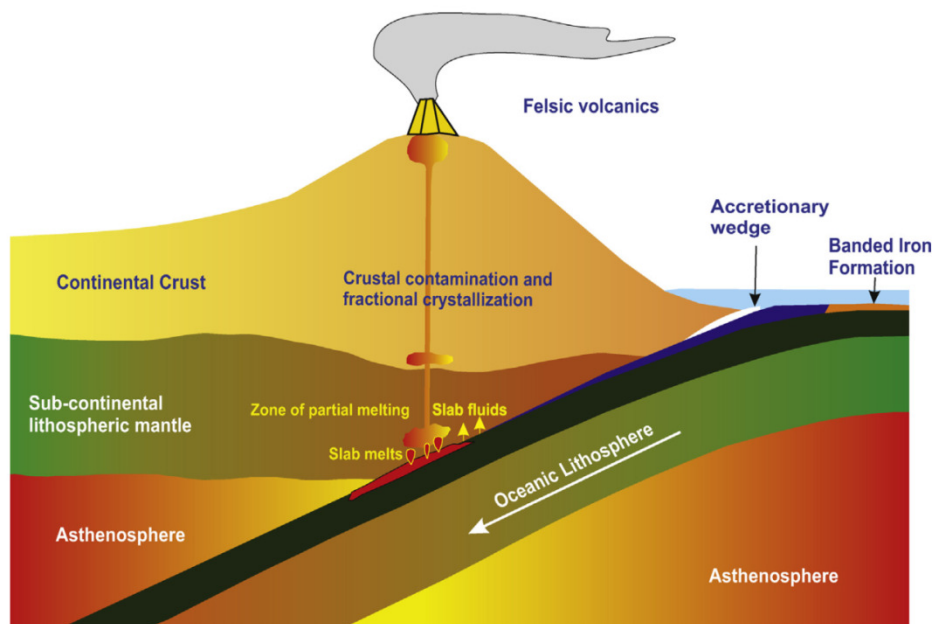


Figure-19: Schematic representation of subduction setting during the evolution of Shimoga Greenstone Belt³¹.

Pressure temperature conditions of mineralization

The average values of Th CO₂ from the histogram of fluid inclusions (H₂O-CO₂ system equation given were used in the MacFlinCor programme to obtain isochors for type-1 and type-2 inclusions (mineralizing fluids)³².

H₂O-CO₂ inclusions provide the best approximation of the P-T-X of the mineralizing fluid³³. The highest homogenization temperature of these inclusions (348°C) could therefore provide a minimum temperature of the original trapping conditions. At this temperature, the isochors of the H₂O-CO₂ inclusions indicate a pressure of approximately 1.7kbar (Figure-10).

Spread of the isochors and pressure data may account for pressure fluctuations, a common feature in the shear zone-hosted gold deposits, in which fluid pressure often exceeds the lithostatic conditions^{34,35}. The homogenization temperature had to be taken as the minimum temperatures of ore formation which is 348°C, and the maximum pressure of 1.75 kb calculated from fluid inclusion isochors. Any mineralized zone controlled by shear zone ore forming fluids act as open system and thus the pressure correction should be addressed. The correction to the homogenization temperature would be roughly 15°C³⁶. Hence, the minimum temperature of formation of gold from mineralizing fluids at Shimoga was 348± 15°C.

Table-2: Fluid inclusion data is determined by measuring each inclusion at a time (Aqueous, aqueous carbonic and carbonic inclusions) from the mineralised zone.

Inc Type	Class	Shape	Size	Fill	Te	Tm _{ice}	Tm _{CO₂}	Th _{CO₂}	Phase	Th _{total}	EqWt% NaCl	Density
V+L	Primary	Irregular	17.18	0.89	-30	-2.5	-56.7	16	Liquid	230	4.07	0.86
V+L	Primary	Faceted	7.52	0.91	-22	-1.5			Liquid	168	2.47	0.92
V+L	Primary	Faceted	4.2	0.73	-20	-1.2			Liquid	162	1.98	0.92
L	Primary	Faceted	1.94				-56.9	15	Liquid			0.82
L	Primary	Irregular	1.1				-56.9	20	Liquid			0.77
L	Primary	Irregular	0.72				-57.2	21	Liquid			0.76
V+L	Secondary	Irregular	11.73	0.91	-32	-12			Liquid	160	15.96	1.03
V+L	Secondary	Irregular	2.52	0.92	-30	-11.5			Liquid	158	15.47	1.02
V+L	Primary	Irregular	4.37	0.88	-25	-0.8			Liquid	168	1.32	0.91
V+L	Primary	Faceted	1.08	0.84	-26	-1.3			Liquid	162	2.14	0.92
V+L	Primary	Irregular	4.88	0.96	-25	-2			Liquid	165	3.28	0.93
V+L	Primary	Faceted	2.28	0.94	-23	-2.2			Liquid	163	3.60	0.93
V+L	Primary	Irregular	4.1	0.95	-27	-3.3			Liquid	170	5.32	0.94
V+L	Primary	Rounded	5.5	0.9	-26	-2.9			Liquid	215	4.70	0.88
V+L	Primary	Rounded	3.91	0.92	-20	-0.9			Liquid	172	1.49	0.91
V+L	Primary	Faceted	0.72	0.82	-18	-0.8			Liquid	170	1.32	0.91
V+L	Primary	Faceted	0.9	0.78	-15	-0.6			Liquid	172	0.99	0.91
V+L	Primary	Faceted	2.61	0.8	-18	-0.5			Liquid	230	0.83	0.83
V+L	Primary	Faceted	5.04	0.77	-21	-3.3	-56.8	28	Liquid	348	5.32	0.68
V+L	Primary	Irregular	5.32	0.71	-22	-3	-56.6	25	Liquid	345	4.86	0.68
V+L	Primary	Faceted	8.25	0.78	-24	-0.9	-56.6	18	Liquid	235	1.49	0.83
V+L	Primary	Irregular	2.2	0.94	-18	-0.3			Liquid	228	0.50	0.83
V+L	Primary	Irregular	2.43	0.91	-20	-0.5			Liquid	230	0.83	0.83
V+L	Primary	Irregular	2.32	0.94	-18	-0.8			Liquid	228	1.32	0.84
V+L	Primary	Irregular	7.75	0.93	-23	-0.5			Liquid	230	0.83	0.83
V+L	Primary	Faceted	3.37	0.91	-20	-0.8			Liquid	228	1.32	0.84
V+L	Primary	Faceted	0.96	0.86	-18	-0.4			Liquid	225	0.66	0.84
V+L	Primary	Faceted	0.99	0.87	-28	-1.2			Liquid	175	1.98	0.91
V+L	Primary	Irregular	2.28	0.91	-27	-1.5			Liquid	170	2.47	0.92
V+L	Primary	Irregular	1.65	0.92	-28	-1.8			Liquid	178	2.96	0.91
V+L	Primary	Irregular	4.62				-56.6	22	Liquid			0.75
V+L	Primary	Irregular	4.2				-56.8	20	Liquid			0.77
V+L	Primary	Irregular	3.78	0.94	-29	-0.9			Liquid	190	1.49	0.89
V+L	Primary	Irregular	1.1	0.88	-30	-1.2			Liquid	185	1.98	0.90
V+L	Primary	Irregular	1.2	0.89	-25	-0.8			Liquid	188	1.32	0.89

Conclusion

Petrographic studies of wafers indicate the presence of primary and secondary mono-phase/bi-phase inclusions in one sample. The characters of the bubble indicate heterogeneous nature of the parent fluid. Any mineralized zone controlled by shear zone ore forming fluids act as open system and thus the pressure correction should be addressed. The highest homogenization temperature of these inclusions (348°C) could therefore provide a minimum temperature of the original trapping conditions. At this temperature, the isochors of the H₂O-CO₂ inclusions indicate a pressure of approximately 1.7kbar. Hence, the minimum temperature of formation of gold from mineralizing fluids study area was 348± 15°C.

Acknowledgements

The authors acknowledge the Dept. of Applied Geology, Kuvempu University for providing the available facilities to carry out this work. The first author also wishes to acknowledge University Grant Commission for providing RGNF fellowship and Dr. Gopal Krishna, Dr. Shariff and Dr. Girish, Mineralogists, PPOD lab, GSI, Bangalore for helping me in obtaining Fluid inclusions data and their encouragement.

References

1. Srikanthappa C. (2001). Deep crustal fluids in the Precambrian rocks of southern India - present study and future investigations in the new millennium. *Indian Mineralogist*, 35, 56-60. ISSN 0019-5928.
2. Radhakrishna B.P. and Vaidyanadhan R. (1997). Geological of Karnataka *Geol. Soc. India*, 353.
3. Harinadha Babu P., Ponnuswamy M. and Krishnamurthy K.V. (1981). Shimoga belt. Early Precambrian supracrustals of southern Karnataka. Geological Survey of India Memoir 112, 199-218.
4. Goldstein R.H. (2003). petrographic analysis of fluid inclusions. insamson i., anderson a. and marshall d. eds., fluid inclusions: Analysis and Interpretation, Mineralogical Association of Canada Short Course, 32, 9-53.
5. Bodnar R.J. (2003). Introduction to fluid inclusions. In I. Samson, A. Anderson, and D. Marshall, Eds., Fluid Inclusions: Analysis and Interpretation, Mineralogical Association of Canada Short Course, 32, 1-8.
6. Radhakrishna B.P. and Curtis L.C. (1999). Gold in India. GSI Publications, 3, 1.
7. Swaminath J., Ramakrishnan M. and Viswanatha M.N. (1976). Dharwar stratigraphic model and Karnataka craton evolution. *Rec GeolSurv India*, 107(2), 149-175.
8. Gillerman V.S. and Sibson R.H. (1987). Comment and Reply on" Earthquake rupturing as a mineralizing agent in hydrothermal systems. *Geology*, 16(7), 669-670.
9. lai Jianqing, JU Peijiao, Tao Jinjin, Yang Baorong and Wang Xiaoyun (2015). Characteristics of Fluid Inclusions and Metallogenesis of Annage Gold Deposit in Qinghai Province, China. Scientific Research Publishing, 5(11), 780-794.
10. Pichumuthu C.S. (1962). Some observation on the structure, metamorphism and geological evolution of peninsular India. *Geological Society of India*, 3, 106-108.
11. Pichumuthu C.S. (1974). Dharwar craton. *Jour. Geol. Soc. India*, 15, 339-346.
12. Pichumuthu C.S. and Srinivasan R. (1983). A billion-year history of the Dharwar craton. *Geol. Soc. India, Mem.*, 4, 121-142.
13. Chadwick B., Ramakrishnan M., Vasudev V.N. and Vishwanatha M.N. (1989). Facies Distribution and structure of Dharwar Volcano-Sedimentary Basin: evidence From Late Archean Transpression in Southern India. *Jour.Geol. Soc.London*, 146, 825-834.
14. Drury, S.A. and Holt, R.W. (1980): The tectonic frame works of the south Indian craton a reconnaissance involving LANDSAT imagery. *Tectonophysics*, 65(3-4), T1-T15.
15. Jayanand M. and Mahabaleswar B. (1991). Relation between shear zones and igneous activity; The closepet granite of southern India. *Proc.Ind.Acad.Sci.*, 100(1), 31-36.
16. Swaminath J. and Ramakrishnan M. (1981). Early Precambrian Supracrustals of Southern Karnataka. Memoir Geological Survey of India, 112, 308.
17. Roedder E. (1984). Fluid inclusions. Mineralogical Society of America, Reviews in Mineralogy, 12, Ed. Ribbe, P.H. 646.
18. Radhakrishna B.P and Curtis L.C. (1991). Gold-the India scene. Geological Society of India, 3(1), 160.
19. Chadwick B. (1994). The Dharwar Supergroup in western Karnataka: A review based on the Babaabudan-Ranibennur tract. *Geo Karnataka, MGD centenary*, 81-94.
20. Radhakrishna B.P. (1996). Mineral resource of Karnataka. Geological Society of India, Min. Res. India, 8, 214-279.
21. Chadwick B., Vasudev V.N., Krishna Rao B. and Hegde G.V. (1991). The stratigraphy and structure of Dharwar super group adjacent to Honnali dome; implication for late Archean basin development in and regional structure in the western part of Karnataka. *Journal, Geological Society of India*, 38(5), 457-484.
22. Chadwick B., Vasudev V.N. and jayaram S. (1988). Stratigraphy and structure of late Archean, Dharwar volcanic and sedimentary rocks and their basement in a part of the Shimoga basin, East of Bhadravathi, Karnataka. *Geological Society of India*, 32(1), 1-19.

23. kerkhof alfons van den, kronz andreas and simon klaus (2014). Deciphering fluid inclusions in high-grade rocks. *Geoscience Frontiers*, 5(5), 683-695.
24. Brown P.E. and Lamb W.M. (1988). P-V-T properties of fluids in the system H₂O-CO₂-NaCl: New graphical presentation and implications for fluid inclusion studies. *Geochim.Cosmochim.Acta*, 53(6), 1209-1221.
25. Kerrick D.M. and Jacobs C.K. (1981). Devolatilisation equilibria in H₂O-CO₂ and H₂O-CO₂ -NaCl fluids: an experimental and thermodynamic evaluation at elevated pressures and temperatures. *American Mineralogist*, Department of Geosciences, 66, 1135-1153.
26. Ganguly Sohini, Manikyamba C., Saha Abhishek, Lingadevaru M., Santosh M., Rambabu S., Arubam C. Khelen, D. Purushotham and Linga D. (2015). Geochemical characteristics of gold bearing boninites and banded iron formations from Shimoga greenstone belt, India: Implications for gold genesis and hydrothermal processes in diverse tectonic settings. *Ore Geology Reviews*, 73, 59-82. Ref- OREGEO1643.
27. Touret J.L.R. (2001). Fluids in metamorphic rocks. *Lithos Journal*, 55, 1-25.
28. Shepherd T.J., Rankin A.H. and Alderton D.H.M. (1985). A practical guide to fluid inclusion studies. Blackie & Son, Glasgow, UK, 239.
29. Cox (1995). Fractures, Fluid Flow and Mineralization. Geological Society of London Science , 54-139.